Vibrational Properties of a Polycrystalline Titanium Surface Studied by Electron Energy-Loss Fine Structure (EELFS) Analysis

Mitsunori Kurahashi, Masahiro Yamamoto*, Mahito Mabuchi* and Shizuo Naito*

National Research Institute for Metals, Tsukuba, Ibaraki 305, Japan
**Institute of Advanced Energy, Kyoto University, Uji, Kyoto 611, Japan*

(Received: Jan. 30, 1997 Accepted: Feb. 21, 1997)

Abstract

We have measured the electron energy loss fine structure (EELFS) of a polycrystalline titanium surface in reflection mode for electron beams at different incidence angles to the normal of the surface. From the analysis of the temperature dependence of the EELFS spectra, we have shown that the mean square relative displacement of the titanium atoms is particularly large on the surface layer and is estimated to be more than twice that for bulk This result is consistent with the reported results of LEED measurements.

1. Introduction

The electron energy loss fine structure (EELFS) is a feature observed at an energy above the core loss edge in electron energy loss spectra. In recent years it has been experimentally and theoretically demonstrated that the EELFS observed in both transmission mode and reflection mode can be analyzed using a formalism similar to that used for the analysis of the extended X-ray absorption fine structure (EXAFS) [1-7].Since the reflection EELFS preferentially gives us information about a surface region owing to the short mean free path of a probe electron, it has been applied to the analysis of surface structures [5,7-13] and surface vibrational properties [13-15], which can be discussed in terms of the radial distribution function (RDF) or the EELFS Debye Waller factor (DWF). In comparison to LEED, EELFS is particularly useful in that it gives us information about the local environment around the atomic species excited by incidence electrons.

Characteristic behavior in surface layers of solids, such as the surface relaxation or the enhanced motion of atoms, are expected to be well investigated from the analysis of the depth dependence of the EELFS RDF or DWF. This is particularly so when we attempt to make clear the difference between the behaviors in the surface and those in the bulk. However, there are only a few reports on such analysis, and to our knowledge no detailed analysis of the depth dependence of the EELFS DWF has been reported. We here consider the EELFS of titanium primarily because it can comparatively easily be measured above the titanium L_{23} edge. Actually measurements of the EELFS of titanium have been reported by some workers [1,11]. No discussion, however, is found about the change in the EELFS measured for electron beams at different incidence angles, which permits an analysis of the depth dependence of the RDF and the EELFS DWF.

In the present study we measure the temperature dependence of the EELFS of a clean titanium surface at different incidence angles. We discuss the change in the interatomic distance and the EELFS DWF with the incidence angle and with the depth from the surface. The result is compared with those obtained from the LEED measurements[16,17].

2. Experimental

All measurements were done in an Ultra-High-Vacuum (UHV) system which had a base pressure of the order of 10^{-8}Pa. The electron energy loss spectra and Auger electron spectra (AES) were obtained by the use of a Varian single-pass cylindrical mirror analyzer with resolution (E/dE) of 200. We measured the derivative electron energy loss spectra using an electron beam with an incident energy E_p of 1800 eV and a current of 1.5 μA. In order to change the penetration depth of incidence electrons, we used the electron beam at four incidence angles θ_i = 20°, 60°, 75° and 80° to the normal of the specimen surface. The modulation voltage was selected to be 10 V peak-to-peak. It took less than 15 min for a single scan. To improve the signal to noise ratio in the spectra, we repeated the measurement 4-

5 times and averaged numerically the collected data.

A polycrystalline titanium foil of dimensions 25mm × 25mm × 0.025mm and 99.95% purity was used as a specimen. It was mechanically polished, ultrasonically degreased in acetone and then spotwelded onto two tantalum support wires of 0.8mm in diameter. In order to clean the surface the specimen was heated resistively by passing an AC current through it. After this heat treatment we found no significant difference in the Auger electron spectra of the titanium surface measured at room temperature and at 373 K-973 K. The temperature of the specimen was measured with a Pt-PtRh13 % thermocouple spotwelded to it and was controlled with a thermoregulator. The fluctuation of the specimen temperature was within ±5 K. The surface of the specimen was again cleaned by repeating Ar^+ ion bombardment (2 keV, 10 $\mu A/cm^2$) at 773 K followed by annealing at 1073 K. We continued this procedure until no segregation of sulfur was observed for the specimen heated to 973 K for more than an hour The cleanliness of the specimen was monitored by AES. When contamination was observed, we momentarily heated the specimen to a high temperature to recover the cleanliness.

We now make a rough estimate of the penetration depth assuming that the probe electron can travel through its attenuation length in titanium metal. The attenuation length for a 1800 eV electron can be estimated to be 23.13 Å by using the formula reported by Seah and Dench[18]. The estimated penetration depth is thus 9.1Å, 5.9Å, 3.8Å and 2.8Å for θ_i = 20°, 60°, 75° and 80°, respectively. These values correspond to 3.9, 2.5, 1.6 and 1.2 monolayers with a spacing of 2.34Å and parallel to the Ti(0001) surface.

3. Method of EELFS Data Analysis

Figure 1 shows the temperature dependence of the electron energy loss spectra for the L_{23} edge of the clean titanium surface that were measured at an incidence angle of 20°. The L_{23} edge is located at an energy loss of 460 eV followed by the EELFS oscillation. The EELFS oscillation of the L_{23} edge was found to decay with increasing temperature, while the shape and intensity of the spectrum of the L_{23} edge to remain unchanged. The structure at 560 eV is

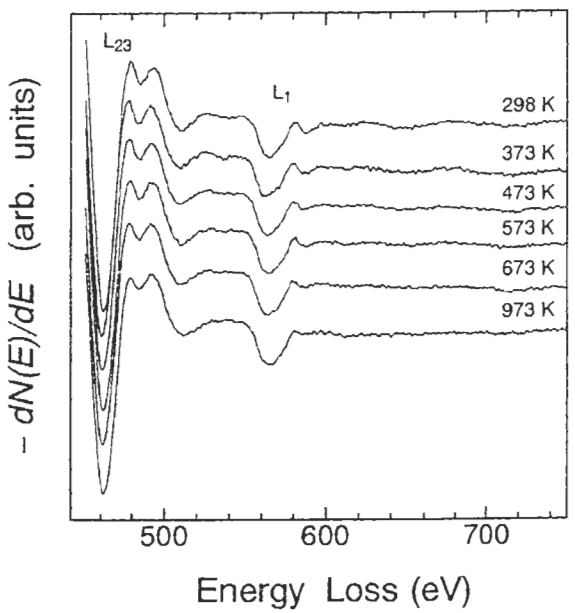

Fig. 1 The electron energy loss spectra of the titanium L_{23} edge measured at the temperatures shown. Measurements were made in first derivative mode at an incident energy E_p = 1.8 keV and the incidence angle $\theta i = 20°$.

due to the ionization of the L_1 edge and overlaps the EELFS oscillation. In order to minimize the influence of the L_1 edge on the analysis of the EELFS oscillation, we normalize the EELFS spectra with respect to the peak-to-peak intensity of the L_{23} edge and subtract from the EELFS spectra the spectrum measured at 973 K. We can ignore the effect of the L_1 edge on the resulting EELFS spectra for the following reasons. First, through the process of the subtraction the structure due to the ionization of the L_1 edge is canceled because its shape and intensity is, as in the case of the L_{23} edge, expected to remain unchanged with temperature. Secondly, the amplitude of the EELFS oscillation originated from the ionization of the L_1 edge is much weaker than that of the L_{23} edge considering the difference of intensities of their thresholds. In the following, we will demonstrate that the results of our analysis, which ignores the effect of the L_1 edge, agree well with the reported results. This supports the assumption that the effect of the L_1 edge is negligible.

Figure 2 shows the EELFS spectra from which the spectrum measured at 973 K has been subtracted. The EELFS spectra are numerically integrated and the background is removed by fitting to them a sixth order polynominal curve.

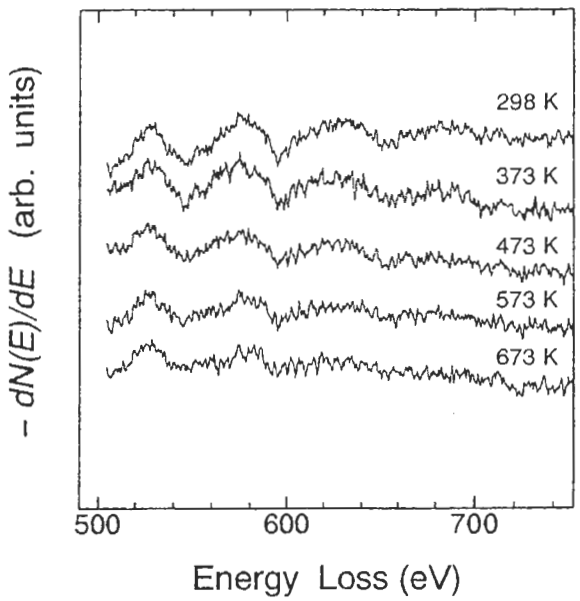

Fig. 2 The electron energy loss spectra subtracted by the spectrum measured at 973 K. The spectra were measured at $\theta i = 20°$and normalized with respect to the L_{23} edge intensity before making subtraction.

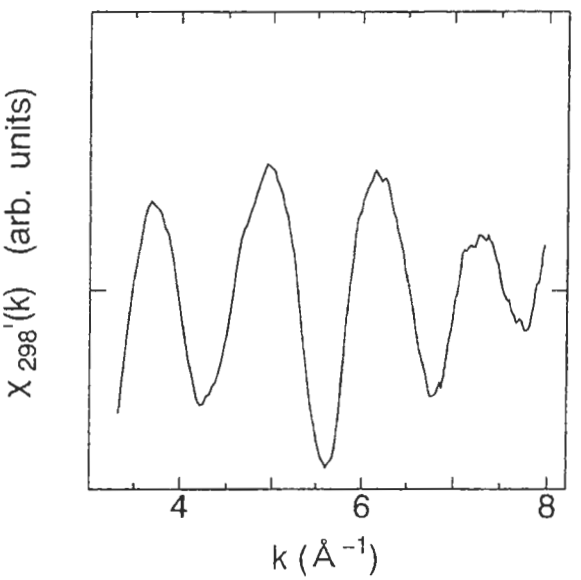

Fig. 3 The EELFS modulation derived from the spectra beyond the titanium L_{23} edge measured at 298 K and $\theta i = 20°$. The k wave vector is referred to the L_{23} edge.

The small change in the order of the fitting polynominal curve has little effects on the shape of the modulating structure obtained. The energy loss is graduated with respect to the onset energy of the L_{23} edge (460 eV) and the spectra are then transformed into k-wave vectors. The modulating structure χ'_{298} (k) is thus isolated and shown in figure 3. The noisy spectrum shown in figure 2 has become the smooth χ'_{298} (k) curve through the process of numerical integration. The maximum and minimum positions of χ'_T (k) are consistent with those in the reported $\chi(k)$ curves of EXAFS[19] and EELFS[1]. It is noted that χ'_T (k) can be written as

$$\chi'_T(k) = \chi_T(k) - \chi_{973}(k) \qquad (1)$$

where $\chi_T(k)$ is the EELFS modulating structure at temperature T.

4. Results and Discussion

4.1 EELFS radial distribution function

We here present the result of the Fourier transform of the EELFS. Following the standard method for EXAFS, we multiply the $\chi_T'(k)$ by k and then Fourier transform it in the range $3.3 < k(Å^{-1}) < 8.0$ using a Henning window function. In figure 4, the magnitude of the Fourier transform ($F'_{298}(r)$) of the $\chi'_{298}(k)$ is shown for θ_i = 20°, 60°, 75° and 80°. The corresponding penetration depth is about 9.1Å, 5.9Å, 3.8Å and 2.8Å. The position of the first peak at *ca.* 2.5 Å is reproducible within 0.06 Å and well agreed with the reported Fourier

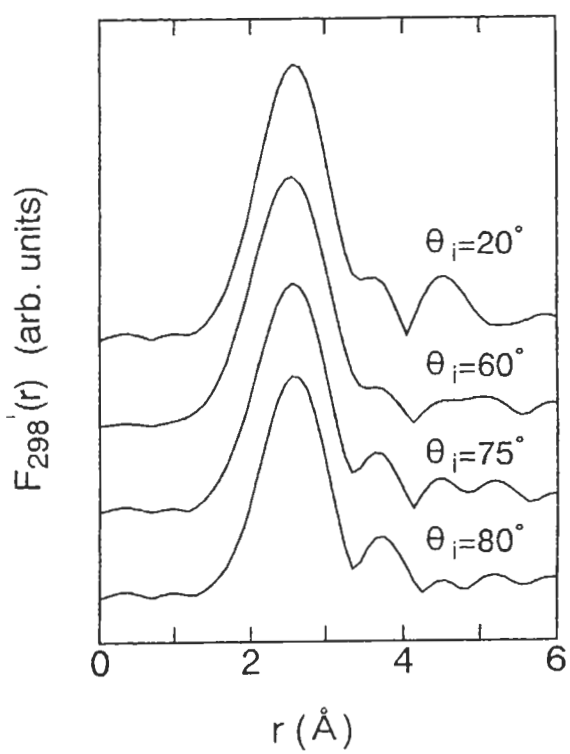

Fig. 4 The magnitudes of Fourier transforms $F'_{298}(r)$ of the EELFS modulation $\chi'_{298}(k)$ obtained from the spectra measured at electron incidence angles shown in the figure.

transform of EXAFS[19] and EELFS[1]. The peaks beyond the second nearest neighbor shell, however, are affected by the ripple resulting from the Fourier integration within the limited k-range. Therefore we will discuss only the first peak in detail.

No difference of the first peak positions of $F'_{298}(r)$ is found, within the experimental error, for the measurements at different incidence angles. This indicates that the change in the interatomic distance between the nearest neighbor (NN) titanium atoms is less than 0.06Å within the depth 9.1Å from the surface. This result is in good agreement with the LEED result by Shih et al. [16]. They showed that the contraction of the interlayer spacing between the outermost layer and the second layer of the Ti(0001) surface was 2% of the interlayer spacing in the bulk and that the interatomic distance between titanium atoms on the outermost layer agreed with that in the bulk. Therefore the contraction in the average distance from an atom on the outermost layer to its NN atoms is estimated to be less than 1% of the interatomic distance, *i.e.* less than 0.03Å, provided that only the outermost layer is excited. If the excitation in the second layer is also considered, the resulting contraction is smaller. Since the contribution from the second layer cannot be neglected even for the measurement at $\theta_i = 80°$ in the present study, we expect no appreciable change in the position of the peak corresponding to the NN atoms.

4.2 EELFS Debye Waller factor

The temperature dependence of Debye Waller Factor (DWF) has been determined based on the ratio method[20]. In the present study this method has been modified as follows. First, the contribution of the first coordination shell to the EELFS modulation has been singled out by backtransforming to the k space the first peak in the RDF. In figure 5, the resulting $k\chi'(k)$ filtered EELFS function ($k\chi'(k)_1$) and its amplitude function are shown for 298 K, 473 K and 673 K. By the use of harmonic approximation[21] the amplitude function $A_T(k)$ is found to be proportion to ($exp[-2\sigma_1^2(T)k^2] - exp[-2\sigma_1^2(973)k^2]$). Here $\sigma_1^2(T)$ is the EELFS DWF for the first coordination shell at temperature T.

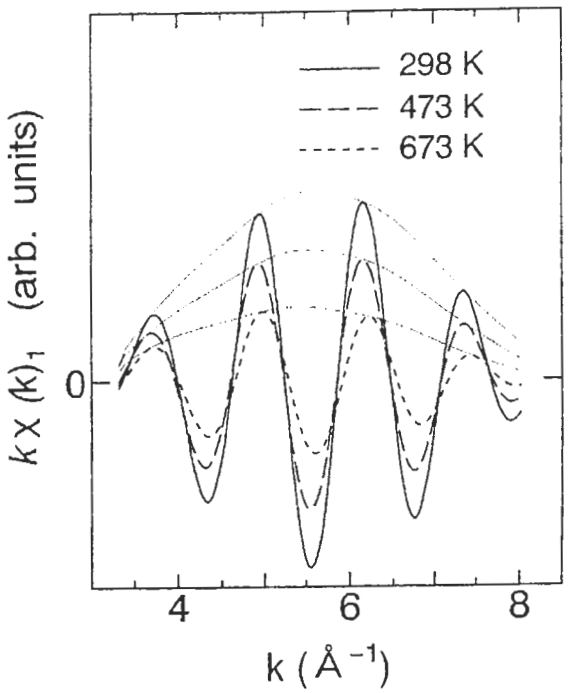

Fig. 5 The Fourier-filtered EELFS functions and the corresponding amplitudes obtained from $\chi'_1(k)$ at $\theta_i = 20°$.

Since the coordination number does not change with temperature, the amplitude ratio can be reduced to

$$\ln\left[\frac{A_T(k)}{A_{298}(k)}\right] = \ln\left(\frac{\exp\left[2\left(\sigma_1^2(973)-\sigma_1^2(T)\right)k^2\right]-1}{\exp\left[2\left(\sigma_1^2(973)-\sigma_1^2(298)\right)k^2\right]-1}\right) \quad (2)$$

Figure 6 shows eq.(2) calculated for 373 K, 473 K, 573 K and 673 K plotted against k^2. The two parameters $\sigma_1^2(973)$- $\sigma_1^2(T)$ and $\sigma_1^2(973)$- $\sigma_1^2(298)$ in eq.(2) have been determined by minimizing the sum of squares of the difference between the values calculated using the experimental result and a fitting function at each temperature.

As shown in figure 6, the overall bahaviour of the the left hand side of eq.(2) is well reproduced by the fitting function. In the following, we will discuss only $\Delta\sigma^2 \equiv \sigma_1^2(T)$- $\sigma_1^2(298)$, which is the difference between the two parameters, because the right hand side of eq.(2) converges to $2(\sigma_1^2(T)$- $\sigma_1^2(298))k^2$ for large k^2 and only the difference of the two parameters is of significance.

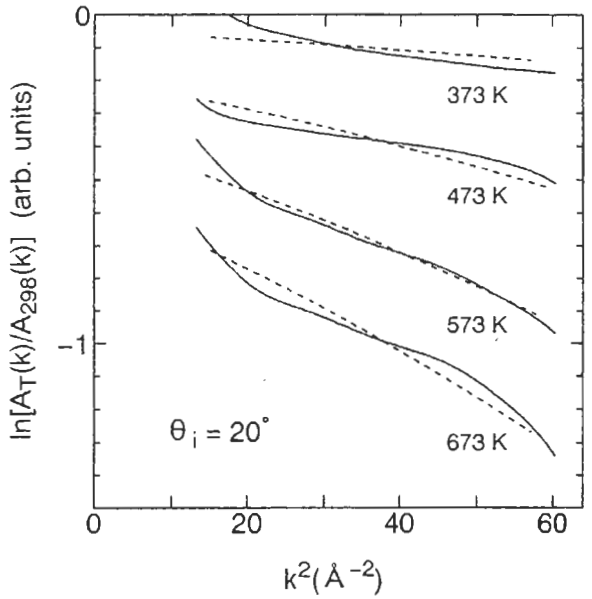

Fig. 6 The ratios of the amplitudes at T = 373 K, 473 K, 573 K and 673 K to the amplitude at 298 K plotted against k^2. The amplitudes have been calculated using the spectra measured at θ_i = 20°. The solid lines are calculated from eq.(2) and the dashed lines show the fitting functions.

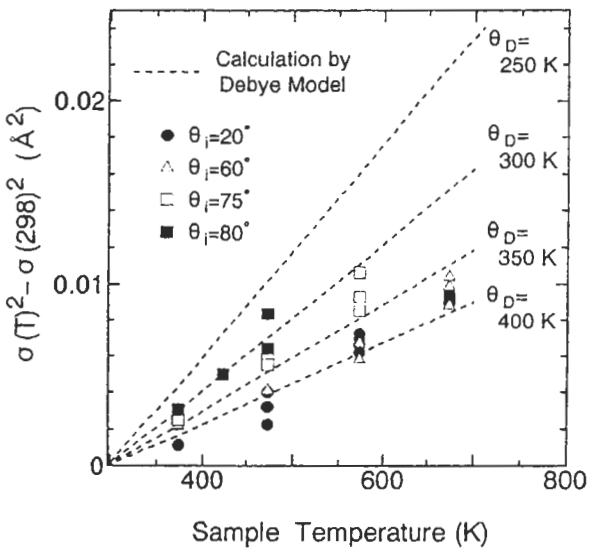

Fig. 7 $\Delta\sigma^2 = \sigma^2_1(T) - \sigma^2_1(298)$ for first coordination shell experimentally obtained at the incidence angles shown. The dashed lines show the calculated $\Delta\sigma^2$ by using eq.(3) at the θ_D values shown.

In figure 7, $\Delta\sigma^2$ is plotted for different θ_i values. The $\Delta\sigma^2$ value is larger for a larger θ_i and for θ_i = 80° it is about twice that for θ_i = 20°. The estimated penetration depth is about 3.9, 2.5, 1.6 and 1.2 monolayers for θ_i =20°, 60°, 75° and 80°, respectively. This result indicates that the $\Delta\sigma^2$ value for the surface layer is much larger than that of the other layers in the polycrystalline titanium. Furthermore, its value can be estimated to be more than twice that for the bulk. In order to compare this result with other experimental results reported, we calculate $\Delta\sigma^2$ using Debye approximation and estimate the Debye temperature θ_D for different incidence angles. As in the EXAFS DWF, the EELFS DWF characterizes the mean square relative displacement (MSRD) and its functional form for the j th coordination shell is given, within Debye approximation, by

$$\sigma_j^2 = \frac{6\hbar}{m\omega_D}\left[\frac{1}{4}+\left(\frac{T}{\theta_D}\right)^2\int_0^{\frac{\theta_D}{T}}\frac{x}{e^x-1}dx\right]-\frac{6\hbar}{m\omega_D}\left[\frac{1-\cos\left(q_D R_j^0\right)}{2\left(q_D R_j^0\right)^2}+\left(\frac{T}{\theta_D}\right)^2\int_0^{\frac{\theta_D}{T}}\frac{\frac{\theta_D}{q_D R_j^0 T}\sin\left(\frac{q_D R_j^0 T x}{\theta_D}\right)}{e^x-1}dx\right] \quad (3)$$

Here, θ_D is the Debye temperature, q_D is the Debye wave vector, m is the atomic mass, k_B is the Boltzmann constant, $\hbar$ is Plank's constant and R_j^0 is the interatomic distance for the j th coordination shell The values of $\Delta\sigma^2$ calculated from eq.(3) are shown for θ_D = 250 K, 300 K, 350 K and 400 K by the dashed lines in figure 7. These values well reproduce the experimental results. The values of θ_D that best reproduce the experimental result are 410±40 K, 380±20 K, 325±20 K and 295±15 K for θ_i = 20°, 60°, 75° and 80°, respectively. The θ_D value for bulk titanium has been reported to lie in the range 342-420 K[17], which is in good agreement with those for θ_i =20° and 60°.

We now compare the EELFS θ_D values estimated above with the effective Debye temperature obtained from the LEED study of the Ti(0001) surface[17]. Since both EELFS and LEED use electrons as a probe, we can discuss the θ_D values in terms of the penetration depth of the electrons. Figure 8 shows a comparison of the EELFS θ_D values and the LEED θ_D values.

The range in which the reported Debye temperature of the bulk titanium is also indicated by the dashed lines. The estimated EELFS θ_D value is consistent with the LEED θ_D value in that both increase as the penetration depth increases. We can observe, however, the tendency of the EELFS θ_D to deviate to larger values at small penetration depths.

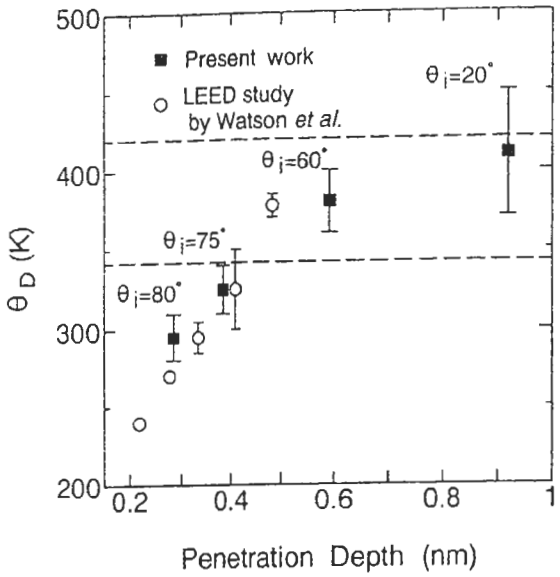

Fig. 8 The Debye temperatures estimated from the EELFS DWF at incidence angles shown and those obtained from the LEED measurement of the Ti(0001) [17] plotted against the penetration depth of the electron. The reported Debye temperature for the bulk lies between the two dashed lines.

In regard to the similarity of the results for the EELFS θ_D and the LEED θ_D mentioned above, we should note the followings. It has been reported that the EELFS DWF parametrizes the MSRD along the direction of the momentum transfer of the incidence electron in the process of the energy loss[13, 15]. Since the direction of momentum transfer can not be specified under the present experimental condition, the estimated EELFS θ_D is expected to include the effect from vibrational components both normal and parallel to the surface.In contrast the LEED θ_D discussed above parametrizes the mean square displacement (MSD) normal to the surface ($<u_\perp^2>$).It has been reported that on clean metal surfaces $<u_\perp^2>$ is larger than the parallel component of the MSD $<u_\parallel^2>$ [23-25] and as the depth from the surface increases, the difference between $<u_\perp^2>$ and $<u_\parallel^2>$ rapidly decreases and they approach the value in the bulk[22]. Therefore the EELFS θ_D and the LEED θ_D are expected to coincide with each other at larger penetration depth, *i.e.* at smaller incidence angles At small penetration depths, however, because of the larger contribution of the $<u_\parallel^2>$ on the surface layer to the EELFS θ_D, the EELFS θ_D is expected to be larger than the LEED θ_D. For a further discussion of the comparison of the EELFS θ_D and the LEED θ_D, the detailed knowledge about $<u_\perp^2>$ and $<u_\parallel^2>$ for various surface planes is needed.

5. Conclusion

We have measured the temperature dependence of the EELFS spectra of a polycrystalline titanium surface with an electron beam at various incidence angles. From the analysis of the measured spectra, we have shown the followings. The change in the interatomic distance with depth from the surface is within the experimental error, *i.e.* less than 0.06 Å. The mean square relative displacement of the titanium atoms is particularly large on the surface layer and is estimated to be more than twice that for the bulk. This result is consistent with that for the LEED measurement.

References

1. De Crescenzi M, Chiarello G, Colavita E and Memeo R 1984 *Phys. Rev.* B **29** 3730
2. De Crescenzi M, Papagno L, Chiarello G, Scarmozzino R, Colavita E, Rosei R and Mobilio S 1981 *Solid. State. Commun.* **40** 613
3. Lozzi L, Passacantando M, Picozzi P, Santucci S, Diociaiuti M and De Crescenzi M 1992 *Solid. State. Commn.* **83** 921
4. Hitchcock A P and Teng C H 1985 *Surf. Sci.* **149** 558
5. De Crescenzi M and Chiarello G 1985 *J. Phys.* C **18** 3595
6. Mira F and Noguera C 1987 *J. Phys.* C **20** 3863
7. De Crescenzi M, Lozzi L, Picozzi P, Santucci S, Benfatto M and Natoli C R 1989 Phys. Rev. B **39** 8409
8. Yikegaki T, Shibata H, Takatoh S, Fujikawa T and Usami S 1990 *Phys. Scr.* **41** 185
9. De Crescenzi M, Antonangeli F, Bellini C and Rosei R 1983 *Phys Rev. Lett.* **50** 1949
10. Caputi L S, Jiang S L, Amoddeo A and Tucci R 1990 *Phys. Rev.* B **41** 8513
11. Idzerda Y U, Williams Ellen D, Einstein T L and Park R L 1987 *Phys. Rev.* B **36** 5941
12. Rosei R, De Crescenzi M, Sette F, Quaresima C, Savoia A and Perfetti P 1983 *Phys. Rev.* B **28** 1161
13. Tyliszczak T, De Crescenzi M and Hitchcock A P 1988 *Phys. Rev.* B **37** 10664
14. De Crescenzi M, Diociaiuti M, Lozzi L, Picozzi P and Santucci S 1987 *Phys. Rev.* B **35** 5997
15. Hitchcock A P and Tyliszczak T 1989

Physica. B **158** 631
16. Shih H D, Jona F, Jepsen D W and Marcus P M 1976 *J Phys.* C **9** 1405
17. Watson P R and Mishenko III J 1987 *Surf. Sci.* **186** 184
18. Seah M P and Dench W A 1979 *Surf. Interf. Anal.* **1** 2
19. Denley D, Williams R S, Perfetti P, Shirley D A and Stohr J 1979 *Phys. Rev.* B **19** 1762
20. Stern E A, Sayers D E and Lytle F W 1975 *Phys. Rev.* B **11** 4836
21. Beni G and Platsmann P M 1976 *Phys. Rev.* B **14** 1514
22. Clark B C, Herman R and Wallis R F 1965 *Phys. Rev.* **139** A860
23. Wallis R F and Cheng D J 1980 *Solid. State. Commun.* **34** 847
24. Smith R J, Hennessy C, Kim M W, Whang C N, Worthington M and Xu Mingde, 1987 *Phys. Rev. Lett.* **58** 702